Volume 27
Number 39
21 October 2025
Pages 6399–6548

CrystEngComm

rsc.li/crystengcomm

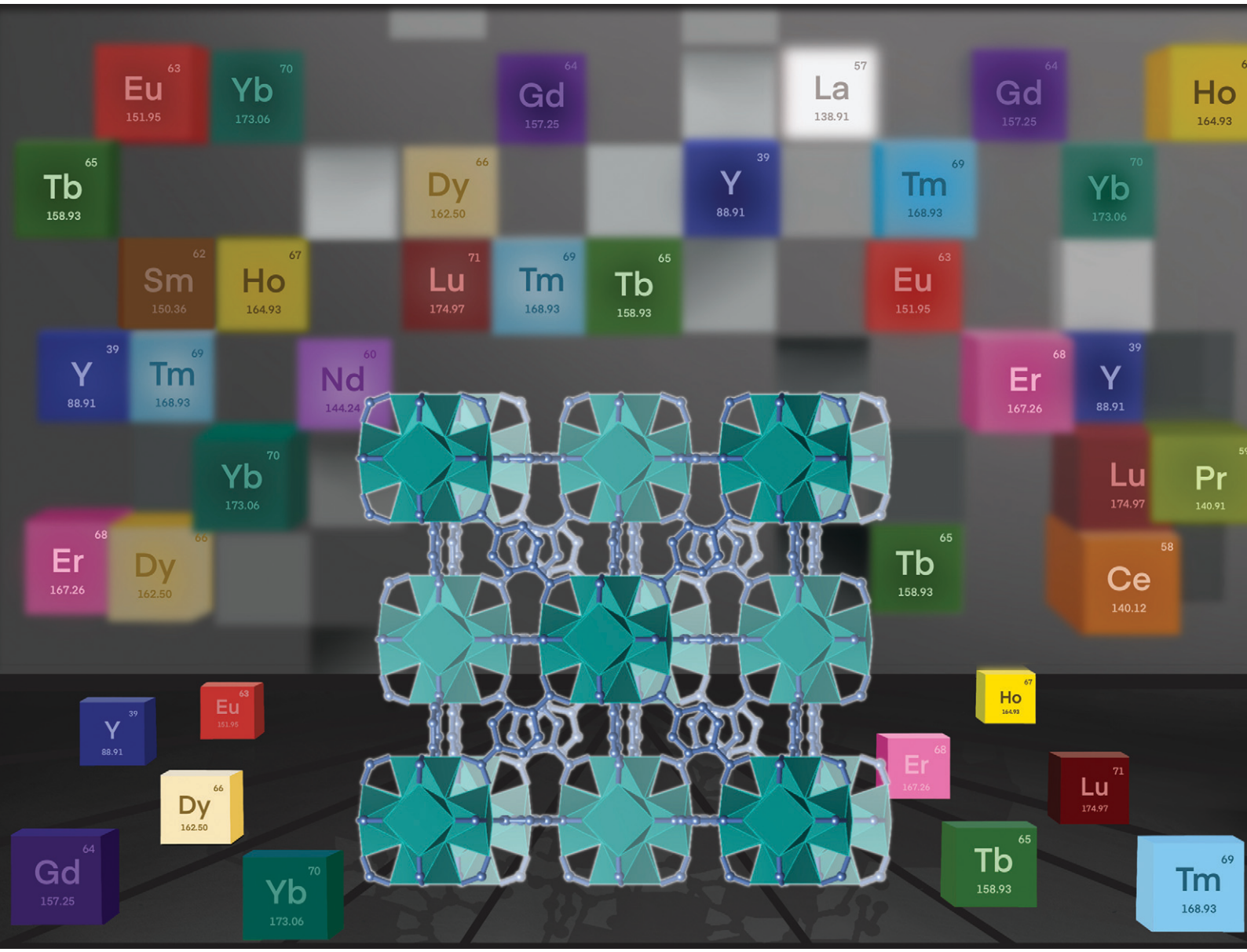

ISSN 1466-8033

ROYAL SOCIETY OF CHEMISTRY

HIGHLIGHT

Ashlee J. Howarth *et al.*
Developments in the discovery, synthesis, and characterization of RE(III)-UiO-66 and its structural analogues

CrystEngComm

HIGHLIGHT

View Article Online
View Journal | View Issue

Cite this: *CrystEngComm*, 2025, **27**, 6406

Developments in the discovery, synthesis, and characterization of RE(III)-UiO-66 and its structural analogues

Micaela Richezzi, [a] P. Rafael Donnarumma[bc] and Ashlee J. Howarth *[a]

Received 22nd July 2025,
Accepted 3rd September 2025

DOI: 10.1039/d5ce00730e

rsc.li/crystengcomm

New metal–organic frameworks (MOFs) are continuously being designed and discovered. As new MOFs emerge in the literature, they are catalogued according to different features, such as the nature of their metal nodes or linkers, structural arrangement, or physical properties, to name a few. In this highlight, developments in the history, synthesis, and characterization of a rare-earth cluster-based MOF with **fcu** net, specifically RE-UiO-66, are discussed including analogues with substituted terephthalic acid linkers. Examples demonstrating the photophysical properties of these MOFs are included to highlight their potential applications related to photoluminescence such as white light emission and temperature sensing.

Introduction

It has been more than 30 years since the important early contributions of Robson,[1] Yaghi,[2–4] Kitagawa,[5] and Férey[6] to the field of metal–organic frameworks (MOFs). MOFs are porous materials with tunable surface area, density, stability, and chemical properties.[7,8] This tunability is a consequence of the high number of synthetic building block combinations that can be used to produce MOFs.[9] Being a subset of coordination polymers and networks, MOFs are mainly crystalline, 2 or 3-dimensional materials with the potential for porosity.[10] Structurally speaking, MOFs are scaffolding-like materials containing inorganic building units (single metal ions, chains, or clusters) connected with each other *via* organic building units (multitopic ligands) called linkers. As a result of their chemical versatility, and in turn their structural tunability, MOFs have been studied for a wide range of applications including, but not limited to, gas adsorption,[11–13] catalysis,[14–16] chemical sensing,[17,18] and water treatment.[19–21]

Reticular chemistry is an approach described by Yaghi and O'Keeffe to design, synthesize, and catalogue MOFs based on their net structures.[22,23] In principle, understanding the geometry and connectivity of the building blocks that compose a MOF with a particular net can be used to create a template to build new MOFs with building blocks that present similar (or the same) geometry and connectivity as the first ones.[24] In the MOF field, these building blocks are represented by the inorganic nodes, and organic linkers, with the former being the main component of the secondary building unit (SBU) of the MOF.[25]

As the number of reported MOFs increased in the 1990s and early 2000s, a procedure became necessary to describe their structures and distinguish them from other closely related systems.[24] For example, in organic chemistry when an alkene is described it is important to denote whether it is the *E*, or the *Z* stereoisomer. The same is true with structures of such complexity as MOFs, wherein a 4-connected net can be represented by multiple descriptors and can take many forms. These representative nets, in the field of MOF chemistry, are given a bolded three-letter code and collected in the Reticular Chemistry Structure Resource (RCSR).[24]

One of these nets is the one described by a single 12-connected vertex (or node), called **fcu** (Fig. 1a).[26] The **fcu** net receives its name from the face-centred cubic unit cell. In the MOF field, the foremost **fcu** net structure is exemplified by Zr-UiO-66 (UiO = University of Oslo, Fig. 1b).[27] Since its original report, in 2008 by Cavka, Lillerud *et al.*,[28] Zr-UiO-66 has attracted the attention of many researchers due to its structural robustness,[29,30] reproducible synthesis,[31] scalability,[32] and application potential.[33–35]

Zr-UiO-66 is most often synthesised solvothermally in *N*,*N*-dimethylformamide (DMF) using terephthalic acid (H_2BDC) and a Zr(IV) salt, from which a hexanuclear cluster forms (Fig. 1b and c).[28,31,36] Other additives, called modulators,[37,38] are often added to the reaction mixture to slow down the Zr(IV)–O(linker) bond formation, allowing for 3-dimensional structure propagation and for some control over defects,[39] crystallinity,[40] or crystal size.[40,41] Zr-UiO-66 has a face centred-cubic unit cell and crystallizes in the $Fm\bar{3}m$ space

[a] *Department of Chemistry and Biochemistry and Centre for NanoScience Research, Concordia University, 7141 Sherbrooke Street West, Montreal, Quebec, H4B 1R6, Canada. E-mail: ashlee.howarth@concordia.ca*
[b] *Soft Matter Nanotechnology Group, CIC biomaGUNE, Basque Research and Technological Alliance, San Sebastian, Spain*
[c] *Departamento de Química Aplicada, Universidad del País Vasco UPV/EHU, Leioa, Bizkaia, Spain*

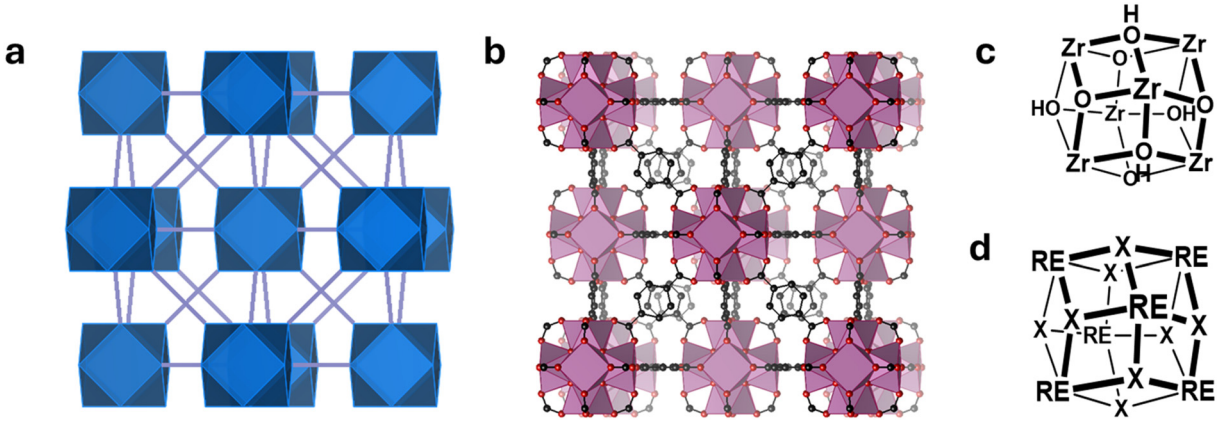

Fig. 1 (a) **fcu** net, (b) structure of UiO-66, (c) $[Zr_6O_4OH_4]^{12+}$ cluster of Zr-UiO-66, and (d) $[RE_6X_8]^{10+}$ cluster of RE-UiO-66, where X = OH or F.

group, with a lattice parameter, *a*, of 20.7 Å. The MOF is comprised of two distinct types of cages, an octahedral one of 12 Å diameter and a tetrahedral cage of 7.5 Å, both with 6 Å apertures (Fig. 1b).[42] As a result of this structure, the calculated theoretical pore volume of Zr-UiO-66 is 0.77 $cm^3\ g^{-1}$, and its surface area is 1160 $m^2\ g^{-1}$.[43]

The **fcu** net of Zr-UiO-66 is defined by a 12-connected node that comes from the inorganic building block – a Zr(IV)-hexanuclear cluster, which is bridged to 12 other clusters through BDC^{2-} linkers.[31] In this hexanuclear cluster, Zr(IV) ions are bridged through hydroxo, or oxo ligands (Fig. 1c). It is the high connectivity of this building block (12), and the strength of the Zr(IV)–O bond that contributes significantly to the high thermal, mechanical, and chemical stability of Zr-UiO-66.[27]

In addition to being an attractive MOF for various applications,[44] Zr-UiO-66 has acted as a structural model for the discovery of a myriad of isoreticular MOFs that have since been described in literature. Structures isoreticular to Zr-UiO-66 with **fcu** net have been reported using different tetravalent metals (Zr(IV),[28] Hf(IV),[45] Ce(IV),[46] Th(IV),[47] U(IV),[48] Pu(IV)[49]) with H_2BDC and many other linear ditopic linkers.[27,46,48,50–52]

An interesting group of metals with versatile coordination chemistry for constructing SBUs for MOFs are the rare-earths (REs) – which include yttrium, scandium, and the series of fifteen lanthanoids.[53] What is interesting about the RE ions, from a structural perspective, is their diverse coordination chemistry with small energetic differences between different coordination numbers and geometries, with the latter being primarily dictated by ligand steric effects.[54] The variability in coordination number and geometry of RE ions adds complexity to structure prediction and synthesis of RE-MOFs, but it also opens the door for the discovery of new structures, comprised of diverse metal nodes,[55–57] sometimes with highly connected nets.[58,59] Moreover, the lanthanoid ions have unique electronic properties dictated by their 4f electron configurations,[60] which contributes to their potential in applications such as sensing,[61] near-infrared emission,[62,63] single molecule magnets,[64] and white-light emission,[65] amongst many others. While these applications are not exclusive to RE-MOFs, they can certainly take advantage of the unique properties of lanthanoids to perform the intended purpose.

In addition to the various tetravalent metal analogues of UiO-66, RE(III) ions can also be used to form the 12-connected hexanuclear cluster required to make UiO-66 isostructures. The first example of RE(III)-hexanuclear clusters being used to synthesize an **fcu** MOF was reported by Xue, Eddaoudi *et al.*[66] They reported seven structures, obtained with Y(III) and Tb(III) using asymmetric heterofunctional ditopic linkers (Fig. 2). Most importantly, Xue, Eddaoudi and coworkers demonstrated that in order to synthesise the RE(III) hexanuclear clusters *in situ*, a fluorinated linker, or modulator, had to be used.[66–68] Since this initial report, the library of RE(III)-based **fcu** MOFs has been in constant expansion.

Synthesis and structure of RE-UiO-66

The first reported RE analogue of UiO-66 was obtained with Ce(IV) and H_2BDC linkers.[46] Like Zr-UiO-66, it is formed by

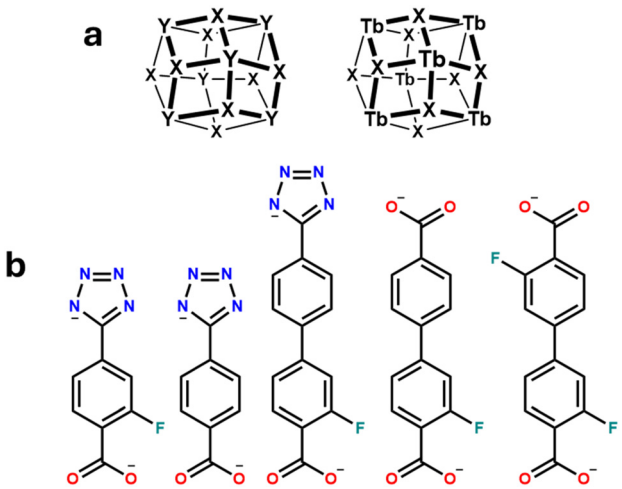

Fig. 2 (a) Clusters and (b) linkers used by Eddaoudi *et al.* to obtain RE(III) **fcu** MOFs.

hexanuclear clusters where the Ce(IV) ions are bridged by μ_3-O and μ_3-OH groups, $[Ce_6O_4(OH)_4]^{12+}$. The synthesis of this MOF does not require fluorinated modulators and can be achieved in short times (15 min) using DMF as a solvent.

While Ce is commonly found in the +4 oxidation state, the other RE ions have a preference for the +3 oxidation state.[69] Although some RE(III)-UiO-66 analogues with substituted BDC^{2-} linkers were reported in 2015,[67] 2017,[70] 2018,[71] 2019 (ref. 72) and 2020,[73] the first synthesis of RE(III)-UiO-66 using non-functionalized BDC^{2-} linkers was reported by our group in 2021.[74] The solvothermal procedure developed to obtain RE-UiO-66 led to eight RE(III) analogues (RE = Y, Eu, Gd, Tb, Ho, Er, Tm, Yb), using the corresponding RE(III) nitrates as precursors and 2,6-difluorobenzoic acid (2,6-dFBA) as the fluorinated modulator. Moreover, we showed that the addition of nitric acid, and the utilisation of dimethylacetamide (DMAc), instead of the more commonly used DMF, led to a more reproducible synthetic procedure for obtaining phase pure RE-UiO-66. In a more recent article, we showed that RE(III) acetates can be used as precursors for the synthesis of RE-UiO-66, in place of RE(III) nitrates.[75] Furthermore, the MOFs synthesized using RE(III) acetates do not present significant differences from those synthesized with RE(III) nitrates in terms of crystallinity, porosity, or overall quality. While RE(III) nitrate precursors are more commonly used for the synthesis of RE(III) cluster-based MOFs, the utilisation of acetates presents advantages such as lower toxicity and hygroscopicity. Avoiding the latter can address issues with synthetic reproducibility attributed to varying humidity conditions in laboratory environments.

In the original article on the synthesis of RE-UiO-66, we solved the structure of the Tm(III) analogue by single-crystal X-ray diffraction (SCXRD), while the other seven analogues were confirmed by powder X-ray diffraction (PXRD).[74] Scanning electron microscopy (SEM) images of RE-UiO-66 show octahedral particles, usually in the range of 1–20 μm. N_2 adsorption–desorption measurements were performed on samples activated at 80 °C under vacuum for 20 h, giving rise to type Ia isotherms, with Brunauer–Emmett–Teller (BET) surface areas in the range 1000–1300 $m^2\ g^{-1}$. It should be noted that we did not observe any evidence of dimethylammonium (DMA) counterions, or capping ligands in our original report on RE-UiO-66, suggesting that the MOFs may have contained defects. However, more recently we have synthesized samples of RE-UiO-66 with DMA counterions and acetate capping ligands (from the decomposition of the DMAc solvent, or from RE(III) acetate precursors), which leads to a decrease in the BET surface areas obtained (650–1230 $m^2\ g^{-1}$).[75]

In 2024, we developed a new procedure to grow larger (~100 μm) single crystals of RE-UiO-66, while also adding Sm-, and Lu-UiO-66 to the library.[74,76] The procedure involves using a solvent mixture DMAc : HCOOH (3 : 1) and using higher temperatures and longer reaction times (140 °C and 4 days). Although it should be noted that the procedure to obtain single crystals does not yield phase pure samples, so should only be used when single crystals are required over bulk microcrystalline powders. RE-UiO-66 crystallizes in the cubic space group $Fm\bar{3}m$. There is one eight-coordinated crystallographically independent RE(III), with a square antiprismatic coordination geometry. The presence of an additional oxygen atom was also observed in a ninth coordination site. While the exact identity of that terminal ligand could not be determined, it is believed to correspond to a coordinated solvent molecule (likely water). The MOF presents the expected octahedral and tetrahedral cages, of 12 and 7 Å, respectively. Using the single crystal X-ray structures obtained for RE-UiO-66 (RE = Lu(III) to Sm(III)), the effect of the ionic radii of the lanthanoids on structural parameters was also studied. We observed an increase in the unit cell parameter when moving from Lu(III) to Sm(III), which is expected due to the increasing ionic radii of the RE(III).[76] Furthermore, a weak linear correlation was found between the thermal stability of the framework and the ionic radii, with Lu-UiO-66 presenting the highest thermal stability, collapsing at 460 °C. On the other hand, Sm-UiO-66 presented a low thermal stability, collapsing at 423 °C. Eu-UiO-66 behaved as an outlier, exhibiting a decomposition temperature lower than expected (400 °C). This latter observation was hypothesized to be due to a transition through a less stable Eu(II) intermediate.[77]

Given that the hexanuclear cluster in the Zr(IV) analogue is bridged by μ_3-O and μ_3-OH,[78] at the time of our first publication on RE-UiO-66 we[74] (and others)[66,67] believed that the RE(III) hexanuclear cluster was bridged by μ_3-OH groups. However, Vizuet, Balkus *et al.*[79] showed that assigning these ligands as μ_3-F groups led to a better crystallographic fit, leading to thermal/displacement ellipsoids and atomic displacement parameters that were larger than the RE sites, as expected. They further confirmed that the RE(III) clusters of Ho-UiO-66 contained fluoro groups by X-ray photoelectron spectroscopy (XPS). Shortly after, Christian, Rimsza *et al.*[80] used DFT calculations to determine that replacing μ_3-OH groups by μ_3-F groups in RE-UiO-66 increases the formation enthalpy of the MOF, resulting in increased stability. Zwanziger, Murugesu *et al.*[81] later evaluated the fluorine content of Y-UiO-66 using solid state ^{19}F nuclear magnetic resonance (NMR) spectroscopy and detected multiple resonances, suggesting a mixture of fluoro and hydroxo groups bridging the cluster.

Unlike the neutral Zr(IV) and Ce(IV)-UiO-66 analogues, the RE(III) analogues are anionic, and a counterion is needed to balance the charge. While DMA, formed by the decomposition of the solvent, was expected to be the counterion, it was not detected in these MOFs until 2024.[75] The counterion can be detected by infrared (IR) spectroscopy and ^1H NMR spectroscopy, with peaks around 3600 cm^{-1} and 2.7 ppm, respectively. In a defect-free MOF, two DMA cations are needed to balance the charge. However, the presence of acetate in the ^1H NMR spectra of many RE-UiO-66 analogues suggests that the MOF is defective. By considering that the

charge should be balanced, the ^{1}H NMR integrations can be used to determine the formula of the MOF, which frequently contains five BDC linkers and the missing linker is capped by acetate ligands. The number of DMA cations in this case is equal to the number of acetate capping ligands.[75] The new formula leads to a % RE that is in agreement with the one obtained from thermogravimetric analysis (TGA). Missing linker and node defects are common for Zr-UiO-66, and have been extensively studied.[82] Defects have not been studied in depth for RE-UiO-66 analogues, and a thorough analysis would require a combination of techniques, such as TGA, N_2 sorption, NMR spectroscopy, inductively coupled plasma mass spectrometry (ICP-MS), XRD, potentiometric titrations, Fourier-transform infrared spectroscopy (FTIR) and Raman spectroscopy.[82]

RE-UiO-66 analogues with substituted terephthalic acid linkers

The first analogue of RE-UiO-66 with substituted linkers was reported by Eddaoudi *et al.*[67] in 2015 using 1,4-naphthalenedicarboxylic acid (H_2NDC, Fig. 3) as the linker and Eu(III), Tb(III), and Y(III) nitrates as precursors. The synthesis was performed using 2-fluorobenzoic acid (2-FBA) as modulator and a solvent mixture of DMF, water, and nitric acid. Similar conditions were used by Han *et al.*[71] in 2018 and Zhang *et al.* in 2020,[73] to obtain analogues with 2-aminoterephthalic (H_2BDC-NH_2) acid and 2-hydroxyterephthalic acid (H_2BDC-OH), respectively.

Another analogue of RE-UiO-66 with substituted H_2BDC linkers was reported by Sava Gallis *et al.*[70] and was obtained by using 2,5-dihydroxyterephthalic acid (H_2DOBDC) as the linker (Fig. 3). RE-UiO-66-$(OH)_2$ or RE-DOBDC was obtained using metal nitrates (RE = Nd, Yb, or Y) or chlorides (RE = Eu) and 2-FBA as a modulator in a mixture of DMF and H_2O. The authors also added nitric acid as a co-modulator to the synthesis of Eu-, Yb- and Y-UiO-66-$(OH)_2$ to improve the crystallinity of the MOFs. In 2021, Nenoff and coworkers[83] reported a larger series of RE(III) analogues of RE-UiO-66-$(OH)_2$ (or RE-DOBDC) using lanthanoids from La(III) to Lu(III). In both reports, the authors noted that the $DOBDC^{2-}$ linker exhibits two distinct binding modes to the RE(III) hexanuclear cluster (Fig. 4). The first is the typical bridging binding, where each oxygen of the carboxylate linker coordinates to adjacent RE(III) ions of the cluster, and the second is a monodentate binding mode, where each oxygen of the carboxylate linker coordinates to the same RE(III) ion. This type of mixed linker binding has only been reported for RE-UiO-66-$(OH)_2$ analogues, suggesting that the –OH functional groups on the H_2BDC linker might play a role in stabilizing the different binding modes.

Reacting Tb(III) nitrate with H_2BDC-NH_2, 2-fluoroterephthalic (H_2BDC-F) acid or 2-bromoterephthalic acid (H_2BDC-Br) (Fig. 3), we reported Tb-UiO-66-NH_2, Tb-UiO-66-F, and Tb-UiO-66-Br by following the original synthetic procedure reported for RE-UiO-66.[84] The three analogues crystallized in the same cubic space group as RE-UiO-66, $Fm\bar{3}m$. All three Tb-UiO-66 analogues presented lower gravimetric surface areas than Tb-UiO-66, as to be expected when using linkers that contain functional groups that block pore apertures and give rise to higher molecular weights.

Du *et al.*[72] reported the synthesis of a Gd(III) MOF containing tetrafluoroterephthalic acid, using 2,2′-bipyridine as a template and water as solvent. In this case, due to the presence of a highly fluorinated linker, no fluorinated modulator was used.

In 2022, Morsali, Hu *et al.* obtained Y-UiO-66-NH_2 by solvent-assisted linker exchange (SALE) and additional linker installation (Fig. 5).[85] First, the authors made a MOF with a **bcu** net containing 8-connected hexanuclear cluster nodes and 3,3-biphenyl dicarboxylic acid linkers. The **bcu** MOF was soaked in a solution of 2-aminoterephthalic acid in DMF at 120 °C. Following the process by ^{1}H NMR spectroscopy, they observed that the linker exchange and additional linker installation was completed after 4 days. By using PXRD and Rietveld refinement the **fcu** net of the resulting MOF was confirmed.

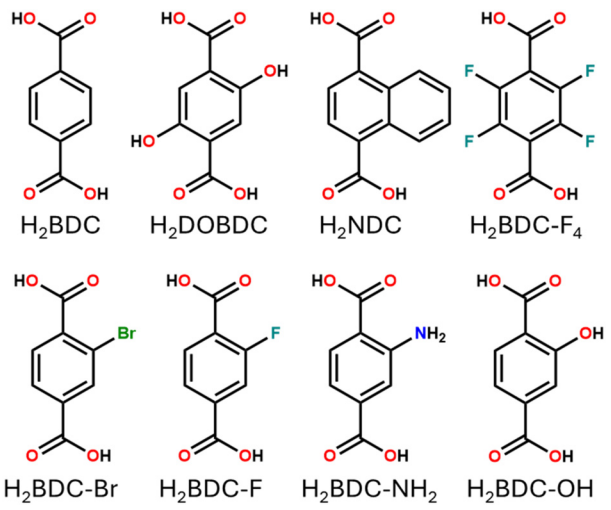

Fig. 3 Linkers used to make RE-UiO-66 analogues.

Photophysical properties of RE-UiO-66

Lanthanoid ions have unique luminescent properties that make lanthanoid-based materials promising for potential

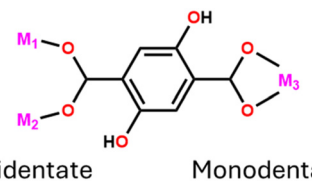

Fig. 4 Scheme of the bidentate and monodentate coordination modes of the DOBDC linker.

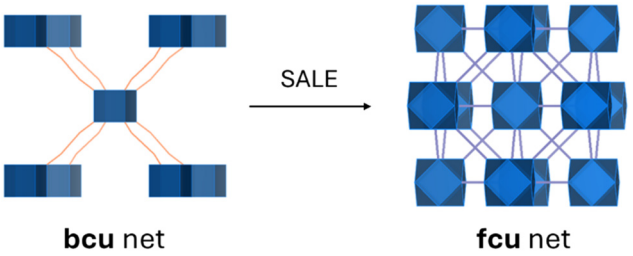

Fig. 5 fcu net obtained from SALE and linker installation on a bcu net.

applications in sensing,[86] bioimaging,[87] and light emitting diodes.[88] While inorganic phosphors containing lanthanoid ions exhibit high quantum yields and exceptional thermal and chemical stability, using these ions in MOF metal nodes combines their unique photophysical properties with the characteristic properties of MOFs. MOFs have some advantages over inorganic phosphors including their tunability, controlled spatial distribution of metal ions that prevents agglomeration, and the much lower temperatures required for their synthesis.[89] However, the lanthanoid ions present the limitation of low molar absorptivity, which leads to weak absorption of photons and subsequent weak luminescence intensity when exciting into the metal.[90] The "antenna effect" arises from using high molar absorptivity chromophores, which, after excitation, transfer energy to the lanthanoid ions 4f excited states.[91–95]

In 2022, we studied the photo- and radioluminescent properties of Tb-UiO-66.[96] When excited at 355 nm into the BDC^{2-} linker, the solid state photoluminescence emission spectrum of Tb-UiO-66 demonstrated the expected green emission bands of Tb(III), corresponding to the transitions $^5D_4 \rightarrow {}^7F_{3,4,5,6}$. The decay time of the $^5D_4 \rightarrow {}^7F_5$ transition in Tb-UiO-66 was found to be 1048.6 ± 6.93 μs, which is typical for Tb(III) f–f transitions. The solid state radioluminescence emission spectrum of Tb-UiO-66 was obtained under 50 kVp and 80 μA unfiltered X-ray excitation, and it also exhibited emissions characteristic of Tb(III). These results suggest that linker-to-metal energy transfer is efficient in Tb-UiO-66, since no linker luminescence was observed in either the photo- or radioluminescence emission spectrum.

The photoluminescent properties of Tb(III) and Eu(III)-UiO-66 analogues with functional groups on the terephthalic acid linker have been reported.[84,97] In the case of Tb-UiO-66 analogues, we carried out calculations to determine the T_1 state energies for various organic linkers (Fig. 6), which included H_2BDC, H_2BDC-F, H_2BDC-Br, H_2BDC-NH_2 and H_2DOBDC.[84] According to Latva's rule, ligand(linker)-to-metal energy transfer is more efficient when the energy difference between the organic linker T_1 excited state to the $^5D_4$ state of Tb(III) is between 2000 and 6000 cm^{-1}.[98] The T_1 state energies of DOBDC and BDC-NH_2 are lower than that of the $^5D_4$ state of Tb(III) (20 500 cm^{-1}), indicating that no Tb(III) emission is expected when exciting into these linkers – a result that was confirmed experimentally. On the other hand, BDC, BDC-F and BDC-Br were able to sensitize the emission of the Tb(III) ion, exhibiting quantum yields (QYs) of 25, 31 and 6%, respectively (before activation). The QY obtained for Tb(III)-UiO-66 is very similar to that reported for an activated Tb(III)-MOF comprised of metal chain nodes and BDC linkers (26%).[99]

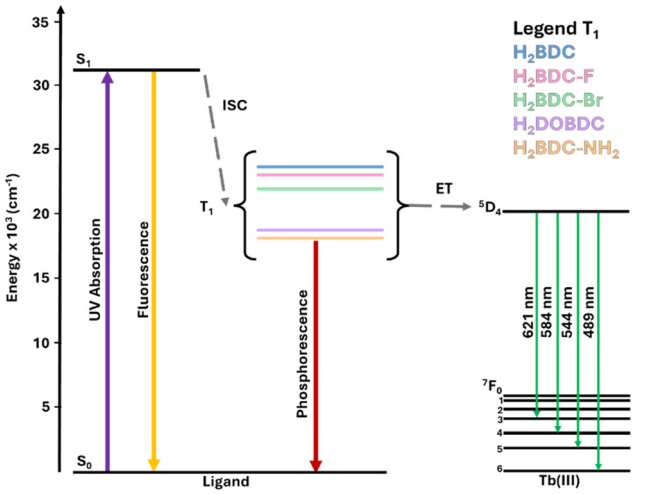

Fig. 6 Energy level diagram depicting the T_1 excited state for the linkers used to synthesize the various analogues of Tb-UiO-66, highlighting the energy transfer from each linker to Tb(III), and the excited state energies of Tb(III).

Xing and coworkers,[97] reported three Eu(III)-UiO-66 analogues using H_2BDC-OH, H_2BDC-NH_2, and H_2NDC as linkers. The photoluminescence emission spectra of the Eu-UiO-66 analogues, when excited at 360 (Eu-NH_2-BDC) and 394 nm (Eu-BDC-OH, Eu-NDC), display a characteristic red emission at 614 nm corresponding to the $^5D_0 \rightarrow {}^7F_2$ transition of Eu(III). Variable-temperature photoluminescence measurements showed that the position of the emission peaks did not change with temperature. However, the three MOFs exhibited stronger emission at lower temperatures, with Eu-BDC-NH_2 presenting a 20.5% enhancement in QY at 140 K, and Eu-BDC-OH and Eu-NDC having their highest enhancements at 170 K (35.9 and 14.9% enhancements, respectively). The photoluminescence QYs at room temperature were found to be 0.35, 1.92 and 5.67% for Eu-BDC-NH_2, Eu-BDC-OH and Eu-NDC, respectively.

Since Gd(III) has higher lying 4f excited states than the other lanthanoids (32 000 cm^{-1} *vs.* <21 000 cm^{-1}), it is rare to find an organic linker that is capable of

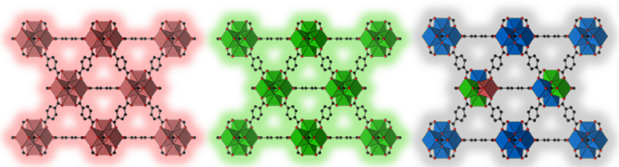

Fig. 7 Structure of Tb-, Eu- and Tb:Gd:Eu-UiO-66 showing the green, red and white emission.

sensitizing Gd(III) emission. As such, Gd-UiO-66 exhibits blue linker-based emission, while Eu- and Tb-UiO-66 present red and green metal-based emission, respectively. The trimetallic Tb:Gd:Eu-UiO-66 analogue can thus be tuned for white light emission (Fig. 7).[100] By tuning the metal ratios in the hexanuclear cluster of RE-UiO-66 to 1.5 : 4.1 : 0.4 (Tb : Gd : Eu), we discovered that cool white light emission could be obtained, with a CIE 1931 colour coordinate of x = 0.3103 and y = 0.3901. The trimetallic MOF exhibited a QY of 11.4% when excited at 312 nm, which is similar to that observed for other white light emitting RE-MOFs. For example, the reported QY for the bimetallic UPC-38($Eu_{0.34}Tb_{0.66}$)-OCH_3 was 13.9%,[101] and a series of Eu(III) doped MOFs with a blue-green emitting ligand exhibited QYs in the range 1–17%.[102]

Temperature sensing is another application that has been studied for RE-UiO-66 and relies on its photophysical properties. In 2018, Feng *et al.*[103] claimed to synthesize bimetallic Eu/Zr-UiO-66 with H_2NDC linkers and used the MOF to prepare thin films. They observed a shift from pink to blue in the emission spectra of the MOF film when the temperature was increased from 237 to 337 K. With the increase in temperature, the linker centred emission intensity decreased to 40% of the initial intensity, while the one based on the Eu(III) ions decreased to 6%. The intensity ratio of Eu(III) to linker emission thus exhibited a negative linear relationship with temperature. The authors reported a relative sensitivity of 4.26 and 2.86% K^{-1} for the films and the powder, respectively. The higher relative sensitivity and strong linear relationship indicate that the films have a superior performance compared to the powder.

In another example, Djanffar, Serier-Brault *et al.*[104] used bimetallic Eu/Tb-UiO-66 for temperature sensing (Fig. 8). In this case, increasing the temperature from 255 to 295 K led to a shift from green to yellow emission, and a 10% quenching was observed for the intensity of Tb(III) while the intensity corresponding to Eu(III) increased by 35%. The relative sensitivity varied with the Tb : Eu ratio, being 4.9 and 3.4% K^{-1} at 295 K for ratios of 5.94 : 0.06 and 5.82 : 0.18, respectively. When the amount of Eu(III) was increased to achieve a Tb : Eu ratio of 5.58 : 0.42, the relative sensitivity reached its maximum at a lower temperature (1.12% K^{-1} at 255 K). The authors suggested that this behaviour could be explained by considering that the probability of obtaining a cluster completely composed of Eu(III) increases in this condition. Therefore, the Tb-to-Eu energy transfer is limited.

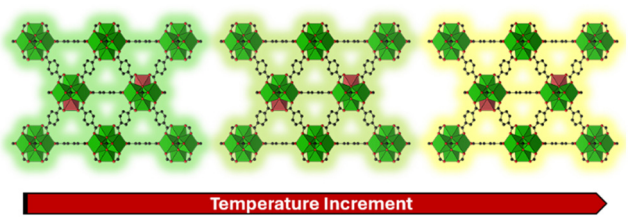

Fig. 8 Shift from green to yellow emission of Eu/Tb-UiO-66 when temperature increases. Green polyhedrons represent Tb atoms, and red Eu.

Schott and collaborators[105] reported a theoretical study of the optical properties of a series of analogues of RE-UiO-66, where RE = La(III), Y(III) and Sc(III). The TD-DFT calculations showed that the absorption properties of these RE-UiO-66 analogues can be modulated by using substituted linkers containing electron-withdrawing groups, such as $-CH_3$, –OH, –SH and $-NH_2$. They also observed that using di-substituted linkers containing –SH and $-NH_2$ groups results in a shift of the absorption to the visible region, which is an interesting result for the potential application of these MOFs in light harvesting under solar irradiation.

Conclusions

Since the discovery of the necessity of fluorinated linkers or modulators to access RE(III)-MOFs containing high nuclearity clusters, numerous RE(III)-MOFs isostructural to UiO-66 have been reported. The RE-UiO-66 analogues have been obtained with eight different linkers and nearly every RE(III) metal, using RE(III) nitrates, chlorides, and acetates as precursors. 2-FBA and 2,6-dFBA are the modulators that are employed to synthesize these MOFs, while DMF and DMAc are the most commonly used solvents, often in combination with water and nitric acid.

Studies on the photophysical properties of the RE-UiO-66 analogues indicate that carefully tuning the composition of RE(III) ions in the cluster nodes or incorporating substituents on the H_2BDC linker can be useful to modulate their photoluminescence. While RE-UiO-66 analogues have been tested for potential applications, like white light emission and temperature sensing, the applications of these MOFs are still underexplored, particularly in comparison to Zr(IV)-UiO-66. Additionally, the development of thin films of RE-UiO-66 would be advantageous for several applications, but due to limitations in the understanding of growth mechanisms and poor structural control,[106] the synthesis of thin films is a challenge, and only a few examples of thin films of RE-UiO-66 analogues can be found in literature.[67]

It is now widely accepted that the hexanuclear clusters in RE-UiO-66 contain a mixture of μ_3-OH and μ_3-F groups, which can be confirmed by SCXRD, XPS, and ^{19}F NMR spectroscopy (solution and solid state) but the exact mechanism leading to the incorporation of μ_3-F groups in these clusters is still not well understood. Furthermore, the nature of defects (*i.e.*, missing linkers and/or nodes) in RE-UiO-66 analogues has not been studied in depth. Given that defects can play an important role in catalysis and gas adsorption, more research will be needed to have a thorough understanding of how best to prepare RE-UiO-66 analogues for these potential applications. Akin to the rich and ever-growing literature on Zr(IV)-UiO-66, we expect to see a continued increase in the study of RE(III)-UiO-66, a similarly fascinating family of MOFs.

Author contributions

Micaela Richezzi: visualization, writing – original draft, writing – review & editing. P. Rafael Donnarumma: visualization, writing – original draft, writing – review & editing. Ashlee J. Howarth: funding acquisition, supervision, writing – review & editing.

Conflicts of interest

No conflicts to declare.

Data availability

This is a highlight review article that discusses research that was published previously by our group and others. Therefore, no new data were generated as part of this manuscript.

Acknowledgements

MR thanks Concordia University for a Graduate Doctoral Fellowship. For our research discussed herein, A. J. H. acknowledges the support of the Natural Sciences and Engineering Research Council of Canada (NSERC) [funding reference number: RGPIN-2018-04388, RGPIN-2024-04293], Cette recherche a été financée par le Conseil de recherches en sciences naturelles et en génie du Canada (CRSNG) [reference numbers: RGPIN-2018-04388, RGPIN-2024-04293], and Fonds de Recherche du Québec – Nature et Technologies, Établissement de la Relève Professorale: 2020-NC-270099. A. J. H. also acknowledges the support of the Concordia University Research Chairs Program.

Notes and references

1 B. F. Hoskins and R. Robson, *J. Am. Chem. Soc.*, 1989, **111**, 5962–5964.
2 O. M. Yaghi, G. Li and H. Li, *Nature*, 1995, **378**, 703–706.
3 O. M. Yaghi and H. Li, *J. Am. Chem. Soc.*, 1995, **117**, 10401–10402.
4 H. Li, M. Eddaoudi, M. O'Keeffe and O. M. Yaghi, *Nature*, 1999, **402**, 276–279.
5 M. Kondo, T. Yoshitomi, H. Matsuzaka, S. Kitagawa and K. Seki, *Angew. Chem., Int. Ed. Engl.*, 1997, **36**, 1725–1727.
6 A. K. Cheetham, G. Férey and T. Loiseau, *Angew. Chem., Int. Ed.*, 1999, **38**, 3268–3292.
7 M. Eddaoudi, J. Kim, N. Rosi, D. Vodak, J. Wachter, M. O'Keeffe and O. M. Yaghi, *Science*, 2002, **295**, 469–472.
8 H. K. Chae, D. Y. Siberio-Pérez, J. Kim, Y. Go, M. Eddaoudi, A. J. Matzger, M. O'keeffe, O. M. Yaghi and M. Design and D. Group, *Nature*, 2004, **427**, 523–527.
9 H. Furukawa, K. E. Cordova, M. O'Keeffe and O. M. Yaghi, *Science*, 2013, **341**, 1230444.
10 S. R. Batten, N. R. Champness, X.-M. Chen, J. Garcia-Martinez, S. Kitagawa, L. Öhrström, M. O'Keeffe, M. P. Suh and J. Reedijk, *CrystEngComm*, 2012, **14**, 3001–3004.
11 S. R. Batten, N. R. Champness, X.-M. Chen, J. Garcia-Martinez, S. Kitagawa, L. Öhrström, M. O'keeffe, M. Paik Suh and J. Reedijk, *Pure Appl. Chem.*, 2013, **85**, 1715–1724.
12 J. A. Mason, M. Veenstra and J. R. Long, *Chem. Sci.*, 2014, **5**, 32–51.
13 S. Ma and H.-C. Zhou, *J. Am. Chem. Soc.*, 2006, **128**, 11734–11735.
14 J. Lee, O. K. Farha, J. Roberts, K. A. Scheidt, S. T. Nguyen and J. T. Hupp, *Chem. Soc. Rev.*, 2009, **38**, 1450–1459.
15 D. Yang and B. C. Gates, *ACS Catal.*, 2019, **9**, 1779–1798.
16 C. Wang, B. An and W. Lin, *ACS Catal.*, 2018, **9**, 130–146.
17 L. E. Kreno, K. Leong, O. K. Farha, M. Allendorf, R. P. Van Duyne and J. T. Hupp, *Chem. Rev.*, 2012, **112**, 1105–1125.
18 C. A. Bauer, T. V. Timofeeva, T. B. Settersten, B. D. Patterson, V. H. Liu, B. A. Simmons and M. D. Allendorf, *J. Am. Chem. Soc.*, 2007, **129**, 7136–7144.
19 A. J. Howarth, Y. Liu, J. T. Hupp and O. K. Farha, *CrystEngComm*, 2015, **17**, 7245–7253.
20 R. J. Drout, L. Robison, Z. Chen, T. Islamoglu and O. K. Farha, *Trends Chem.*, 2019, **1**, 304–317.
21 P. A. Kobielska, A. J. Howarth, O. K. Farha and S. Nayak, *Coord. Chem. Rev.*, 2018, **358**, 92–107.
22 O. M. Yaghi, M. O'Keeffe, N. W. Ockwig, H. K. Chae, M. Eddaoudi and J. Kim, *Nature*, 2003, **423**, 705–714.
23 O. M. Yaghi, *J. Am. Chem. Soc.*, 2016, **138**(48), 15507–15509.
24 M. O'keeffe, M. A. Peskov, S. J. Ramsden and O. M. Yaghi, *Acc. Chem. Res.*, 2008, **41**, 1782–1789.
25 M. Eddaoudi, D. B. Moler, H. Li, B. Chen, T. M. Reineke, M. O'keeffe and O. M. Yaghi, *Acc. Chem. Res.*, 2001, **34**, 319–330.
26 A. H. Assen, K. Adil, K. E. Cordova and Y. Belmabkhout, *Coord. Chem. Rev.*, 2022, **468**, 214644.
27 J. Winarta, B. Shan, S. M. Mcintyre, L. Ye, C. Wang, J. Liu and B. Mu, *Cryst. Growth Des.*, 2019, **20**, 1347–1362.
28 J. H. Cavka, S. Jakobsen, U. Olsbye, N. Guillou, C. Lamberti, S. Bordiga and K. P. Lillerud, *J. Am. Chem. Soc.*, 2008, **130**, 13850–13851.
29 A. M. Hastings, M. Fairley, M. C. Wasson, D. Campisi, A. Sarkar, Z. C. Emory, K. Brunson, D. B. Fast, T. Islamoglu and M. Nyman, *Chem. Mater.*, 2022, **34**, 8403–8417.
30 J. B. DeCoste, G. W. Peterson, H. Jasuja, T. G. Glover, Y.-g. Huang and K. S. Walton, *J. Mater. Chem. A*, 2013, **1**, 5642–5650.
31 M. J. Katz, Z. J. Brown, Y. J. Colón, P. W. Siu, K. A. Scheidt, R. Q. Snurr, J. T. Hupp and O. K. Farha, *Chem. Commun.*, 2013, **49**, 9449–9451.
32 R. T. Jerozal, T. A. Pitt, S. N. MacMillan and P. J. Milner, *J. Am. Chem. Soc.*, 2023, **145**, 13273–13283.
33 F. Vermoortele, B. Bueken, G. Le Bars, B. Van de Voorde, M. Vandichel, K. Houthoofd, A. Vimont, M. Daturi, M. Waroquier and V. Van Speybroeck, *J. Am. Chem. Soc.*, 2013, **135**, 11465–11468.
34 M. J. Katz, J. E. Mondloch, R. K. Totten, J. K. Park, S. T. Nguyen, O. K. Farha and J. T. Hupp, *Angew. Chem.*, 2014, **126**, 507–511.
35 C. Chen, D. Chen, S. Xie, H. Quan, X. Luo and L. Guo, *ACS Appl. Mater. Interfaces*, 2017, **9**, 41043–41054.
36 C. A. Trickett, K. J. Gagnon, S. Lee, F. Gándara, H. B. Bürgi and O. M. Yaghi, *Angew. Chem., Int. Ed.*, 2015, **54**, 11162–11167.

37 S. Hermes, T. Witte, T. Hikov, D. Zacher, S. Bahnmüller, G. Langstein, K. Huber and R. A. Fischer, *J. Am. Chem. Soc.*, 2007, **129**, 5324–5325.
38 R. S. Forgan, *Chem. Sci.*, 2020, **11**, 4546–4562.
39 L. Yuan, M. Tian, J. Lan, X. Cao, X. Wang, Z. Chai, J. K. Gibson and W. Shi, *Chem. Commun.*, 2018, **54**, 370–373.
40 A. Schaate, P. Roy, A. Godt, J. Lippke, F. Waltz, M. Wiebcke and P. Behrens, *Chem. – Eur. J.*, 2011, **17**, 6643–6651.
41 Y. Zhao, Q. Zhang, Y. Li, R. Zhang and G. Lu, *ACS Appl. Mater. Interfaces*, 2017, **9**, 15079–15085.
42 L. Valenzano, B. Civalleri, S. Chavan, S. Bordiga, M. H. Nilsen, S. Jakobsen, K. P. Lillerud and C. Lamberti, *Chem. Mater.*, 2011, **23**, 1700–1718.
43 P. Ghosh, Y. J. Colón and R. Q. Snurr, *Chem. Commun.*, 2014, **50**, 11329–11331.
44 D. Zou and D. Liu, *Mater. Today Chem.*, 2019, **12**, 139–165.
45 S. Jakobsen, D. Gianolio, D. S. Wragg, M. H. Nilsen, H. Emerich, S. Bordiga, C. Lamberti, U. Olsbye, M. Tilset and K. P. Lillerud, *Phys. Rev. B: Condens. Matter Mater. Phys.*, 2012, **86**, 125429.
46 M. Lammert, M. T. Wharmby, S. Smolders, B. Bueken, A. Lieb, K. A. Lomachenko, D. D. Vos and N. Stock, *Chem. Commun.*, 2015, **51**, 12578–12581.
47 C. Falaise, J.-S. Charles, C. Volkringer and T. Loiseau, *Inorg. Chem.*, 2015, **54**, 2235–2242.
48 C. Falaise, C. Volkringer, J. F. Vigier, N. Henry, A. Beaurain and T. Loiseau, *Chem. – Eur. J.*, 2013, **19**, 5324–5331.
49 A. M. Hastings, D. Ray, W. Jeong, L. Gagliardi, O. K. Farha and A. E. Hixon, *J. Am. Chem. Soc.*, 2020, **142**, 9363–9371.
50 Z. Hu, Y. Peng, Z. Kang, Y. Qian and D. Zhao, *Inorg. Chem.*, 2015, **54**, 4862–4868.
51 R. C. Klet, Y. Liu, T. C. Wang, J. T. Hupp and O. K. Farha, *J. Mater. Chem. A*, 2016, **4**, 1479–1485.
52 Z. J. Li, Y. Ju, H. Lu, X. Wu, X. Yu, Y. Li, X. Wu, Z. H. Zhang, J. Lin and Y. Qian, *Chem. – Eur. J.*, 2021, **27**, 1286–1291.
53 F. Saraci, V. Quezada-Novoa, P. R. Donnarumma and A. J. Howarth, *Chem. Soc. Rev.*, 2020, **49**, 7949–7977.
54 M. Seitz, A. G. Oliver and K. N. Raymond, *J. Am. Chem. Soc.*, 2007, **129**, 11153–11160.
55 V. Quezada-Novoa, H. M. Titi, A. A. Sarjeant and A. J. Howarth, *Chem. Mater.*, 2021, **33**, 4163–4169.
56 V. Quezada-Novoa, H. M. Titi, F. Y. Villanueva, M. W. Wilson and A. J. Howarth, *Small*, 2023, **19**, 2302173.
57 J. J. Pang, Z. Q. Yao, K. Zhang, Q. W. Li, Z. X. Fu, R. Zheng, W. Li, J. Xu and X. H. Bu, *Angew. Chem., Int. Ed.*, 2023, **62**, e202217456.
58 V. Guillerm, Ł. J. Weseliński, Y. Belmabkhout, A. J. Cairns, V. D'elia, Ł. Wojtas, K. Adil and M. Eddaoudi, *Nat. Chem.*, 2014, **6**, 673–680.
59 D. Alezi, A. M. P. Peedikakkal, Ł. J. Weseliński, V. Guillerm, Y. Belmabkhout, A. J. Cairns, Z. Chen, Ł. Wojtas and M. Eddaoudi, *J. Am. Chem. Soc.*, 2015, **137**, 5421–5430.
60 S. Fordham, X. Wang, M. Bosch and H.-C. Zhou, *Lanthanide Metal-Organic Frameworks*, 2015, pp. 1–27.
61 Y. Cui, H. Xu, Y. Yue, Z. Guo, J. Yu, Z. Chen, J. Gao, Y. Yang, G. Qian and B. Chen, *J. Am. Chem. Soc.*, 2012, **134**, 3979–3982.
62 K. A. White, D. A. Chengelis, K. A. Gogick, J. Stehman, N. L. Rosi and S. Petoud, *J. Am. Chem. Soc.*, 2009, **131**, 18069–18071.
63 L. L. da Luz, R. Milani, J. F. Felix, I. R. Ribeiro, M. Talhavini, B. A. Neto, J. Chojnacki, M. O. Rodrigues and S. A. Junior, *ACS Appl. Mater. Interfaces*, 2015, **7**, 27115–27123.
64 L. H. Kalinke, D. Cangussu, M. Mon, R. Bruno, E. Tiburcio, F. Lloret, D. Armentano, E. Pardo and J. Ferrando-Soria, *Inorg. Chem.*, 2019, **58**, 14498–14506.
65 J. C. G. Bünzli, *Eur. J. Inorg. Chem.*, 2017, **2017**, 5058–5063.
66 D.-X. Xue, A. J. Cairns, Y. Belmabkhout, L. Wojtas, Y. Liu, M. H. Alkordi and M. Eddaoudi, *J. Am. Chem. Soc.*, 2013, **135**, 7660–7667.
67 D.-X. Xue, Y. Belmabkhout, O. Shekhah, H. Jiang, K. Adil, A. J. Cairns and M. Eddaoudi, *J. Am. Chem. Soc.*, 2015, **137**, 5034–5040.
68 O. Yassine, O. Shekhah, A. H. Assen, Y. Belmabkhout, K. N. Salama and M. Eddaoudi, *Angew. Chem.*, 2016, **128**, 16111–16115.
69 R. E. Connick, *J. Chem. Soc.*, 1949, S235–S241.
70 D. F. Sava Gallis, L. E. S. Rohwer, M. A. Rodriguez, M. C. Barnhart-Dailey, K. S. Butler, T. S. Luk, J. A. Timlin and K. W. Chapman, *ACS Appl. Mater. Interfaces*, 2017, **9**, 22268–22277.
71 Y. Zhang, Y. Wang, L. Liu, N. Wei, M.-L. Gao, D. Zhao and Z.-B. Han, *Inorg. Chem.*, 2018, **57**, 2193–2198.
72 W. Wei, X. Wang, K. Zhang, C.-B. Tian and S.-W. Du, *Cryst. Growth Des.*, 2018, **19**, 55–59.
73 T. Xia, Y. Wan, Y. Li and J. Zhang, *Inorg. Chem.*, 2020, **59**, 8809–8817.
74 P. R. Donnarumma, S. Frojmovic, P. Marino, H. A. Bicalho, H. M. Titi and A. J. Howarth, *Chem. Commun.*, 2021, **57**, 6121–6124.
75 M. Richezzi, P. R. Donnarumma, C. Copeman and A. J. Howarth, *Chem. Commun.*, 2024, **60**, 5173–5176.
76 P. R. Donnarumma, C. Copeman, M. Richezzi, J. Sardilli, H. M. Titi and A. J. Howarth, *Cryst. Growth Des.*, 2024, **24**, 1619–1625.
77 A. Glasner, E. Levy and M. Steinberg, *J. Inorg. Nucl. Chem.*, 1963, **25**, 1415–1422.
78 N. Planas, J. E. Mondloch, S. Tussupbayev, J. Borycz, L. Gagliardi, J. T. Hupp, O. K. Farha and C. J. Cramer, *J. Phys. Chem. Lett.*, 2014, **5**, 3716–3723.
79 J. P. Vizuet, M. L. Mortensen, A. L. Lewis, M. A. Wunch, H. R. Firouzi, G. T. McCandless and K. J. Balkus, Jr., *J. Am. Chem. Soc.*, 2021, **143**, 17995–18000.
80 M. S. Christian, K. J. Fritzsching, J. A. Harvey, D. F. Sava Gallis, T. M. Nenoff and J. M. Rimsza, *JACS Au*, 2022, **2**, 1889–1898.
81 C. Zwanziger, W. D. do Pim, A. A. Kitos, J. S. Ovens, P. J. Pallister and M. Murugesu, *Chem. Commun.*, 2022, **58**, 12700–12703.

82 Y. Feng, Q. Chen, M. Jiang and J. Yao, *Ind. Eng. Chem. Res.*, 2019, **58**, 17646–17659.
83 S. E. Henkelis, D. J. Vogel, P. C. Metz, N. R. Valdez, M. A. Rodriguez, D. X. Rademacher, S. Purdy, S. J. Percival, J. M. Rimsza, K. Page and T. M. Nenoff, *ACS Appl. Mater. Interfaces*, 2021, **13**, 56337–56347.
84 X. A. Canales Galvez, M. Richezzi, H. A. Bicalho, N. Labadie, S. C. Pellegrinet, H. M. Titi and A. J. Howarth, *Inorg. Chem.*, 2025, **64**, 1853–1859.
85 H. Ghasempour, B. Habibi, F. Zarekarizi, A. Morsali and M. L. Hu, *Inorg. Chem.*, 2022, **61**, 16221–16227.
86 J. Dong, D. Zhao, Y. Lu and W.-Y. Sun, *J. Mater. Chem. A*, 2019, **7**, 22744–22767.
87 C. Liu, S. V. Eliseeva, T.-Y. Luo, P. F. Muldoon, S. Petoud and N. L. Rosi, *Chem. Sci.*, 2018, **9**, 8099–8102.
88 Y. Cui, B. Chen and G. Qian, *Coord. Chem. Rev.*, 2014, **273**, 76–86.
89 D. F. Sava Gallis, L. E. Rohwer, M. A. Rodriguez and T. M. Nenoff, *Chem. Mater.*, 2014, **26**, 2943–2951.
90 T. N. Nguyen, F. M. Ebrahim and K. C. Stylianou, *Coord. Chem. Rev.*, 2018, **377**, 259–306.
91 M. D. Allendorf, C. A. Bauer, R. Bhakta and R. Houk, *Chem. Soc. Rev.*, 2009, **38**, 1330–1352.
92 J.-C. G. Bünzli and C. Piguet, *Chem. Soc. Rev.*, 2005, **34**, 1048–1077.
93 K.-L. Wong, J.-C. G. Bünzli and P. A. Tanner, *J. Lumin.*, 2020, **224**, 117256.
94 A. J. Amoroso and S. J. Pope, *Chem. Soc. Rev.*, 2015, **44**, 4723–4742.
95 J. M. Lehn, *Angew. Chem., Int. Ed. Engl.*, 1990, **29**, 1304–1319.
96 Z. Ajoyan, G. A. Mandl, P. R. Donnarumma, V. Quezada-Novoa, H. A. Bicalho, H. M. Titi, J. A. Capobianco and A. J. Howarth, *ACS Mater. Lett.*, 2022, **4**, 1025–1031.
97 L. Chen, Y. Cao, R. Ma, H. Cao, X. Chen, K. Lin, Q. Li, J. Deng, C. Liu, Y. Wang, L. Huang and X. Xing, *Chem. Sci.*, 2024, **15**, 3721–3729.
98 M. Latva, H. Takalo, V.-M. Mukkala, C. Matachescu, J. C. Rodríguez-Ubis and J. Kankare, *J. Lumin.*, 1997, **75**, 149–169.
99 C. Daiguebonne, N. Kerbellec, O. Guillou, J.-C. Bünzli, F. Gumy, L. Catala, T. Mallah, N. Audebrand, Y. Gérault and K. Bernot, *Inorg. Chem.*, 2008, **47**, 3700–3708.
100 Z. Ajoyan, H. A. Bicalho, P. R. Donnarumma, A. Antanovich and A. J. Howarth, *J. Mater. Chem. C*, 2023, **11**, 8929–8934.
101 Y. Wang, K. Zhang, X. Wang, X. Xin, X. Zhang, W. Fan, B. Xu, F. Dai and D. Sun, *J. Mater. Chem. C*, 2020, **8**, 1374–1379.
102 A. E. Psalti, D. Andriotou, S. A. Diamantis, A. Chatz-Giachia, A. Pournara, M. J. Manos, A. Hatzidimitriou and T. Lazarides, *Inorg. Chem.*, 2022, **61**, 11959–11972.
103 J. F. Feng, T. F. Liu, J. Shi, S. Y. Gao and R. Cao, *ACS Appl. Mater. Interfaces*, 2018, **10**, 20854–20861.
104 E. Djanffar, H. A. Bicalho, Z. Ajoyan, A. J. Howarth and H. Serier-Brault, *J. Mater. Chem. C*, 2024, **12**, 8024–8029.
105 Y. Hidalgo-Rosa, M. Saavedra-Torres, B. D. Koivisto, M. A. Treto-Suárez, D. Páez-Hernández, X. Zarate and E. Schott, *J. Mater. Sci.*, 2023, **58**, 8862–8877.
106 C. Crivello, S. Sevim, O. Graniel, C. Franco, S. Pané, J. Puigmartí-Luis and D. Muñoz-Rojas, *Mater. Horiz.*, 2021, **8**, 168–178.